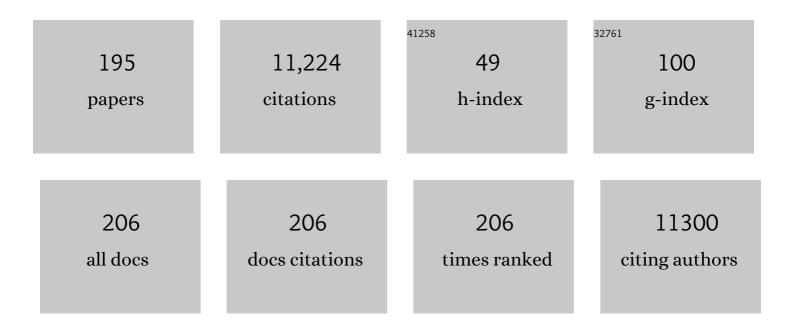


List of Publications by Year in descending order

Source: https://exaly.com/author-pdf/8672337/publications.pdf Version: 2024-02-01



I E VII

| # | Article | IF | CITATIONS |
|----|---|------|-----------|
| 1 | Finer resolution observation and monitoring of global land cover: first mapping results with Landsat TM and ETM+ data. International Journal of Remote Sensing, 2013, 34, 2607-2654. | 1.3 | 1,263 |
| 2 | Stable classification with limited sample: transferring a 30-m resolution sample set collected in 2015 to mapping 10-m resolution global land cover in 2017. Science Bulletin, 2019, 64, 370-373. | 4.3 | 761 |
| 3 | Managing nitrogen to restore water quality in China. Nature, 2019, 567, 516-520. | 13.7 | 667 |
| 4 | Formation of Onionâ€Like NiCo ₂ S ₄ Particles via Sequential Ionâ€Exchange for Hybrid Supercapacitors. Advanced Materials, 2017, 29, 1605051. | 11.1 | 539 |
| 5 | Coordination Polymers Derived General Synthesis of Multishelled Mixed Metalâ€Oxide Particles for Hybrid Supercapacitors. Advanced Materials, 2017, 29, 1605902. | 11.1 | 345 |
| 6 | Deep Learning Based Oil Palm Tree Detection and Counting for High-Resolution Remote Sensing Images. Remote Sensing, 2017, 9, 22. | 1.8 | 284 |
| 7 | General Formation of MS (M = Ni, Cu, Mn) Boxâ€inâ€Box Hollow Structures with Enhanced Pseudocapacitive Properties. Advanced Functional Materials, 2014, 24, 7440-7446. | 7.8 | 281 |
| 8 | China's urban expansion from 1990 to 2010 determined with satellite remote sensing. Science Bulletin, 2012, 57, 2802-2812. | 1.7 | 265 |
| 9 | Google Earth as a virtual globe tool for Earth science applications at the global scale: progress and perspectives. International Journal of Remote Sensing, 2012, 33, 3966-3986. | 1.3 | 257 |
| 10 | Mapping global urban boundaries from the global artificial impervious area (GAIA) data. Environmental Research Letters, 2020, 15, 094044. | 2.2 | 240 |
| 11 | Global urban expansion offsets climate-driven increases in terrestrial net primary productivity. Nature Communications, 2019, 10, 5558. | 5.8 | 198 |
| 12 | Spatial multi-objective land use optimization: extensions to the non-dominated sorting genetic algorithm-II. International Journal of Geographical Information Science, 2011, 25, 1949-1969. | 2.2 | 176 |
| 13 | Towards automatic lithological classification from remote sensing data using support vector machines. Computers and Geosciences, 2012, 45, 229-239. | 2.0 | 162 |
| 14 | Automated mapping of soybean and corn using phenology. ISPRS Journal of Photogrammetry and Remote Sensing, 2016, 119, 151-164. | 4.9 | 156 |
| 15 | Towards a common validation sample set for global land-cover mapping. International Journal of Remote Sensing, 2014, 35, 4795-4814. | 1.3 | 154 |
| 16 | Improving 30Âm global land-cover map FROM-GLC with time series MODIS and auxiliary data sets: a segmentation-based approach. International Journal of Remote Sensing, 2013, 34, 5851-5867. | 1.3 | 146 |
| 17 | Detailed dynamic land cover mapping of Chile: Accuracy improvement by integrating multi-temporal data. Remote Sensing of Environment, 2016, 183, 170-185. | 4.6 | 146 |
| 18 | Stacked Autoencoder-based deep learning for remote-sensing image classification: a case study of African land-cover mapping. International Journal of Remote Sensing, 2016, 37, 5632-5646. | 1.3 | 142 |

| # | Article | IF | CITATIONS |
|----|--|-----|-----------|
| 19 | Semantic Segmentation-Based Building Footprint Extraction Using Very High-Resolution Satellite Images and Multi-Source GIS Data. Remote Sensing, 2019, 11, 403. | 1.8 | 135 |
| 20 | Meta-discoveries from a synthesis of satellite-based land-cover mapping research. International Journal of Remote Sensing, 2014, 35, 4573-4588. | 1.3 | 130 |
| 21 | A fast and fully automatic registration approach based on point features for multi-source remote-sensing images. Computers and Geosciences, 2008, 34, 838-848. | 2.0 | 129 |
| 22 | FROM-GC: 30 m global cropland extent derived through multisource data integration. International Journal of Digital Earth, 2013, 6, 521-533. | 1.6 | 123 |
| 23 | A multi-resolution global land cover dataset through multisource data aggregation. Science China Earth Sciences, 2014, 57, 2317-2329. | 2.3 | 116 |
| 24 | The 2020 China report of the Lancet Countdown on health and climate change. Lancet Public Health, The, 2021, 6, e64-e81. | 4.7 | 106 |
| 25 | The first all-season sample set for mapping global land cover with Landsat-8 data. Science Bulletin, 2017, 62, 508-515. | 4.3 | 104 |
| 26 | Mapping global land cover in 2001 and 2010 with spatial-temporal consistency at 250m resolution. ISPRS Journal of Photogrammetry and Remote Sensing, 2015, 103, 38-47. | 4.9 | 99 |
| 27 | Quantization of the coupling mechanism between eco-environmental quality and urbanization from multisource remote sensing data. Journal of Cleaner Production, 2021, 321, 128948. | 4.6 | 98 |
| 28 | Large-Scale Oil Palm Tree Detection from High-Resolution Satellite Images Using Two-Stage Convolutional Neural Networks. Remote Sensing, 2019, 11, 11. | 1.8 | 93 |
| 29 | Oxygen vacancy-enriched MoO _{3â^'x} nanobelts for asymmetric supercapacitors with excellent room/low temperature performance. Journal of Materials Chemistry A, 2019, 7, 13205-13214. | 5.2 | 92 |
| 30 | Growing status observation for oil palm trees using Unmanned Aerial Vehicle (UAV) images. ISPRS Journal of Photogrammetry and Remote Sensing, 2021, 173, 95-121. | 4.9 | 91 |
| 31 | A systematic sensitivity analysis of constrained cellular automata model for urban growth simulation based on different transition rules. International Journal of Geographical Information Science, 2014, 28, 1317-1335. | 2.2 | 79 |
| 32 | Integrating Google Earth imagery with Landsat data to improve 30-m resolution land cover mapping. Remote Sensing of Environment, 2020, 237, 111563. | 4.6 | 79 |
| 33 | A new research paradigm for global land cover mapping. Annals of GIS, 2016, 22, 87-102. | 1.4 | 77 |
| 34 | Cost-effective priorities for the expansion of global terrestrial protected areas: Setting post-2020 global and national targets. Science Advances, 2020, 6, . | 4.7 | 76 |
| 35 | Assessing the Impacts of Extreme Agricultural Droughts in China Under Climate and Socioeconomic Changes. Earth's Future, 2018, 6, 689-703. | 2.4 | 72 |
| 36 | Tracking annual cropland changes from 1984 to 2016 using time-series Landsat images with a change-detection and post-classification approach: Experiments from three sites in Africa. Remote Sensing of Environment, 2018, 218, 13-31. | 4.6 | 71 |

| # | Article | IF | CITATIONS |
|----|---|-----|-----------|
| 37 | Progress and Trends in the Application of Google Earth and Google Earth Engine. Remote Sensing, 2021, 13, 3778. | 1.8 | 71 |
| 38 | Mapping geochemical singularity using multifractal analysis: Application to anomaly definition on stream sediments data from Funin Sheet, Yunnan, China. Journal of Geochemical Exploration, 2010, 104, 1-11. | 1.5 | 69 |
| 39 | A cellular automata downscaling based 1 km global land use datasets (2010–2100). Science Bulletin, 2016, 61, 1651-1661. | 4.3 | 68 |
| 40 | Green Spaces as an Indicator of Urban Health: Evaluating Its Changes in 28 Mega-Cities. Remote Sensing, 2017, 9, 1266. | 1.8 | 67 |
| 41 | Annual 30-m land use/land cover maps of China for 1980–2015 from the integration of AVHRR, MODIS and Landsat data using the BFAST algorithm. Science China Earth Sciences, 2020, 63, 1390-1407. | 2.3 | 64 |
| 42 | Identifying patterns and hotspots of global land cover transitions using the ESA CCI Land Cover dataset. Remote Sensing Letters, 2018, 9, 972-981. | 0.6 | 63 |
| 43 | How does urban expansion interact with cropland loss? A comparison of 14 Chinese cities from 1980 to 2015. Landscape Ecology, 2021, 36, 243-263. | 1.9 | 62 |
| 44 | An Overview of the Applications of Earth Observation Satellite Data: Impacts and Future Trends. Remote Sensing, 2022, 14, 1863. | 1.8 | 61 |
| 45 | A generalization of spatial and temporal fusion methods for remotely sensed surface parameters. International Journal of Remote Sensing, 2015, 36, 4411-4445. | 1.3 | 56 |
| 46 | Distribution of ecological restoration projects associated with land use and land cover change in China and their ecological impacts. Science of the Total Environment, 2022, 825, 153938. | 3.9 | 56 |
| 47 | A segment derived patch-based logistic cellular automata for urban growth modeling with heuristic rules. Computers, Environment and Urban Systems, 2017, 65, 140-149. | 3.3 | 53 |
| 48 | Multi-scale evaluation of light use efficiency in MODIS gross primary productivity for croplands in the Midwestern United States. Agricultural and Forest Meteorology, 2015, 201, 111-119. | 1.9 | 51 |
| 49 | Cross-regional oil palm tree counting and detection via a multi-level attention domain adaptation network. ISPRS Journal of Photogrammetry and Remote Sensing, 2020, 167, 154-177. | 4.9 | 51 |
| 50 | A Production Efficiency Model-Based Method for Satellite Estimates of Corn and Soybean Yields in the Midwestern US. Remote Sensing, 2013, 5, 5926-5943. | 1.8 | 50 |
| 51 | Long-Term Annual Mapping of Four Cities on Different Continents by Applying a Deep Information Learning Method to Landsat Data. Remote Sensing, 2018, 10, 471. | 1.8 | 50 |
| 52 | Annual oil palm plantation maps in Malaysia and Indonesia from 2001 to 2016. Earth System Science Data, 2020, 12, 847-867. | 3.7 | 50 |
| 53 | Comparison of country-level cropland areas between ESA-CCI land cover maps and FAOSTAT data. International Journal of Remote Sensing, 2018, 39, 6631-6645. | 1.3 | 49 |
| 54 | Towards the automatic selection of optimal seam line locations when merging optical remote-sensing images. International Journal of Remote Sensing, 2012, 33, 1000-1014. | 1.3 | 45 |

| # | Article | IF | CITATIONS |
|----|--|-----|-----------|
| 55 | Design of multiple electrode structures based on nano Ni ₃ S ₂ and carbon nanotubes for high performance supercapacitors. Journal of Materials Chemistry A, 2019, 7, 7406-7414. | 5.2 | 45 |
| 56 | Comparisons of three recent moderate resolution African land cover datasets: CGLS-LC100, ESA-S2-LC20, and FROM-GLC-Africa30. International Journal of Remote Sensing, 2019, 40, 6185-6202. | 1.3 | 43 |
| 57 | Oil palm mapping using Landsat and PALSAR: a case study in Malaysia. International Journal of Remote Sensing, 2016, 37, 5431-5442. | 1.3 | 41 |
| 58 | The 2021 China report of the Lancet Countdown on health and climate change: seizing the window of opportunity. Lancet Public Health, The, 2021, 6, e932-e947. | 4.7 | 41 |
| 59 | Monitoring surface mining belts using multiple remote sensing datasets: A global perspective. Ore Geology Reviews, 2018, 101, 675-687. | 1.1 | 40 |
| 60 | High resolution crop intensity mapping using harmonized Landsat-8 and Sentinel-2 data. Journal of Integrative Agriculture, 2019, 18, 2883-2897. | 1.7 | 40 |
| 61 | A multiple crop model ensemble for improving broad-scale yield prediction using Bayesian model averaging. Field Crops Research, 2017, 211, 114-124. | 2.3 | 39 |
| 62 | Exploring Annual Urban Expansions in the Guangdong-Hong Kong-Macau Greater Bay Area: Spatiotemporal Features and Driving Factors in 1986–2017. Remote Sensing, 2020, 12, 2615. | 1.8 | 39 |
| 63 | A 30 m terrace mapping in China using Landsat 8 imagery and digital elevation model based on the Google Earth Engine. Earth System Science Data, 2021, 13, 2437-2456. | 3.7 | 39 |
| 64 | Geographic stacking: Decision fusion to increase global land cover map accuracy. ISPRS Journal of Photogrammetry and Remote Sensing, 2015, 103, 57-65. | 4.9 | 38 |
| 65 | Rapid corn and soybean mapping in US Corn Belt and neighboring areas. Scientific Reports, 2016, 6, 36240. | 1.6 | 38 |
| 66 | A Circa 2010 Thirty Meter Resolution Forest Map for China. Remote Sensing, 2014, 6, 5325-5343. | 1.8 | 37 |
| 67 | Long-Term Post-Disturbance Forest Recovery in the Greater Yellowstone Ecosystem Analyzed Using Landsat Time Series Stack. Remote Sensing, 2016, 8, 898. | 1.8 | 37 |
| 68 | The Evaluation of SMAP Enhanced Soil Moisture Products Using High-Resolution Model Simulations and In-Situ Observations on the Tibetan Plateau. Remote Sensing, 2018, 10, 535. | 1.8 | 37 |
| 69 | Comparison of the Spatial Characteristics of Four Remotely Sensed Leaf Area Index Products over China: Direct Validation and Relative Uncertainties. Remote Sensing, 2018, 10, 148. | 1.8 | 35 |
| 70 | Long-Term Land Cover Dynamics (1986–2016) of Northeast China Derived from a Multi-Temporal Landsat Archive. Remote Sensing, 2019, 11, 599. | 1.8 | 35 |
| 71 | Investigation of land surface phenology detections in shrublands using multiple scale satellite data. Remote Sensing of Environment, 2021, 252, 112133. | 4.6 | 35 |
| 72 | Mapping finerâ€resolution land surface emissivity using Landsat images in China. Journal of Geophysical Research D: Atmospheres, 2017, 122, 6764-6781. | 1.2 | 34 |

| # | Article | IF | CITATIONS |
|----|---|-----|-----------|
| 73 | Multi-scale habitat selection by two declining East Asian waterfowl species at their core spring stopover area. Ecological Indicators, 2018, 87, 127-135. | 2.6 | 34 |
| 74 | Global-Scale Associations of Vegetation Phenology with Rainfall and Temperature at a High Spatio-Temporal Resolution. Remote Sensing, 2014, 6, 7320-7338. | 1.8 | 33 |
| 75 | Land cover mapping and data availability in critical terrestrial ecoregions: A global perspective with Landsat thematic mapper and enhanced thematic mapper plus data. Biological Conservation, 2015, 190, 34-42. | 1.9 | 33 |
| 76 | Mapping the maximum extents of urban green spaces in 1039 cities using dense satellite images. Environmental Research Letters, 2021, 16, 064072. | 2.2 | 32 |
| 77 | The divergent response of vegetation phenology to urbanization: A case study of Beijing city, China. Science of the Total Environment, 2022, 803, 150079. | 3.9 | 30 |
| 78 | Contrasting Effects of Temperature and Precipitation on Vegetation Greenness along Elevation Gradients of the Tibetan Plateau. Remote Sensing, 2020, 12, 2751. | 1.8 | 29 |
| 79 | FROM-GLC Plus: toward near real-time and multi-resolution land cover mapping. GIScience and Remote Sensing, 2022, 59, 1026-1047. | 2.4 | 29 |
| 80 | Monitoring cropland changes along the Nile River in Egypt over past three decades (1984–2015) using remote sensing. International Journal of Remote Sensing, 2017, 38, 4459-4480. | 1.3 | 27 |
| 81 | Spatial distribution of usable biomass feedstock and technical bioenergy potential in China. GCB Bioenergy, 2020, 12, 54-70. | 2.5 | 27 |
| 82 | Mapping oil palm extent in Malaysia using ALOS-2 PALSAR-2 data. International Journal of Remote Sensing, 2018, 39, 432-452. | 1.3 | 26 |
| 83 | Fire enhances forest degradation within forest edge zones in Africa. Nature Geoscience, 2021, 14, 479-483. | 5.4 | 26 |
| 84 | Circa 2014 African land-cover maps compatible with FROM-GLC and GLC2000 classification schemes based on multi-seasonal Landsat data. International Journal of Remote Sensing, 2016, 37, 4648-4664. | 1.3 | 25 |
| 85 | A multiple dataset approach for 30-m resolution land cover mapping: a case study of continental Africa. International Journal of Remote Sensing, 2018, 39, 3926-3938. | 1.3 | 25 |
| 86 | Oil palm plantation mapping from high-resolution remote sensing images using deep learning. International Journal of Remote Sensing, 2020, 41, 2022-2046. | 1.3 | 25 |
| 87 | An all-season sample database for improving land-cover mapping of Africa with two classification schemes. International Journal of Remote Sensing, 2016, 37, 4623-4647. | 1.3 | 24 |
| 88 | Awareness of Sustainable Development Goals among Students from a Chinese Senior High School. Education Sciences, 2021, 11, 458. | 1.4 | 24 |
| 89 | Annual dynamic dataset of global cropping intensity from 2001 to 2019. Scientific Data, 2021, 8, 283. | 2.4 | 24 |
| 90 | Global urbanicity is associated with brain and behaviour in young people. Nature Human Behaviour, 2022, 6, 279-293. | 6.2 | 24 |

| # | Article | IF | CITATIONS |
|-----|--|-----|-----------|
| 91 | A global map of planting years of plantations. Scientific Data, 2022, 9, 141. | 2.4 | 24 |
| 92 | Aggregative model-based classifier ensemble for improving land-use/cover classification of Landsat TM Images. International Journal of Remote Sensing, 2014, 35, 1481-1495. | 1.3 | 23 |
| 93 | Assessment of the cropland classifications in four global land cover datasets: A case study of Shaanxi Province, China. Journal of Integrative Agriculture, 2017, 16, 298-311. | 1.7 | 23 |
| 94 | Towards global oil palm plantation mapping using remote-sensing data. International Journal of Remote Sensing, 2018, 39, 5891-5906. | 1.3 | 23 |
| 95 | A Real-Time Tree Crown Detection Approach for Large-Scale Remote Sensing Images on FPGAs. Remote Sensing, 2019, 11, 1025. | 1.8 | 23 |
| 96 | Improving Landsat ETM+ Urban Area Mapping via Spatial and Angular Fusion With MISR Multi-Angle Observations. IEEE Journal of Selected Topics in Applied Earth Observations and Remote Sensing, 2012, 5, 101-109. | 2.3 | 22 |
| 97 | Scaling up spring phenology derived from remote sensing images. Agricultural and Forest Meteorology, 2018, 256-257, 207-219. | 1.9 | 21 |
| 98 | Precision medicine and global mental health. The Lancet Global Health, 2019, 7, e32. | 2.9 | 21 |
| 99 | One-third of lands face high conflict risk between biodiversity conservation and human activities in China. Journal of Environmental Management, 2021, 299, 113449. | 3.8 | 21 |
| 100 | Assessing spatiotemporal variations and predicting changes in ecosystem service values in the Guangdong–Hong Kong–Macao Greater Bay Area. ClScience and Remote Sensing, 2022, 59, 184-199. | 2.4 | 21 |
| 101 | Ten years after Hurricane Katrina: monitoring recovery in New Orleans and the surrounding areas using remote sensing. Science Bulletin, 2016, 61, 1460-1470. | 4.3 | 20 |
| 102 | High Resolution Mapping of Cropping Cycles by Fusion of Landsat and MODIS Data. Remote Sensing, 2017, 9, 1232. | 1.8 | 20 |
| 103 | Wrapping RGO/MoO2/carbon textile as supercapacitor electrode with enhanced flexibility and areal capacitance. Electrochimica Acta, 2018, 282, 784-791. | 2.6 | 20 |
| 104 | A fine-resolution estimation of the biomass resource potential across China from 2020 to 2100. Resources, Conservation and Recycling, 2022, 176, 105944. | 5.3 | 19 |
| 105 | A 30 meter land cover mapping of China with an efficient clustering algorithm CBEST. Science China Earth Sciences, 2014, 57, 2293-2304. | 2.3 | 18 |
| 106 | Using a global reference sample set and a cropland map for area estimation in China. Science China Earth Sciences, 2017, 60, 277-285. | 2.3 | 18 |
| 107 | Evaluation of the Common Land Model (CoLM) from the Perspective of Water and Energy Budget Simulation: Towards Inclusion in CMIP6. Atmosphere, 2017, 8, 141. | 1.0 | 18 |
| 108 | The spatial-temporal patterns of land cover changes due to mining activities in the Darling Range, Western Australia: A Visual Analytics Approach. Ore Geology Reviews, 2019, 108, 23-32. | 1.1 | 18 |

| # | Article | IF | CITATIONS |
|-----|--|---------------------|-----------|
| 109 | Assessment of the potential and distribution of an energy crop at 1-km resolution from 2010 to 2100 in China – The case of sweet sorghum. Applied Energy, 2019, 239, 395-407. | 5.1 | 18 |
| 110 | Significant Land Contributions to Interannual Predictability of East Asian Summer Monsoon Rainfall. Earth's Future, 2021, 9, e2020EF001762. | 2.4 | 18 |
| 111 | A 1 km global cropland dataset from 10 000 BCE to 2100 CE. Earth System Science Data, 2021 | , a.3 , 5403 | 3-Бя421. |
| 112 | Deep convolutional neural network based large-scale oil palm tree detection for high-resolution remote sensing images. , 2017, , . | | 17 |
| 113 | Assessing spectral indices to estimate the fraction of photosynthetically active radiation absorbed by the vegetation canopy. International Journal of Remote Sensing, 2018, 39, 8022-8040. | 1.3 | 17 |
| 114 | Estimating the Aboveground Biomass for Planted Forests Based on Stand Age and Environmental Variables. Remote Sensing, 2019, 11, 2270. | 1.8 | 17 |
| 115 | Mapping oil palm plantation expansion in Malaysia over the past decade (2007–2016) using ALOS-1/2 PALSAR-1/2 data. International Journal of Remote Sensing, 2019, 40, 7389-7408. | 1.3 | 17 |
| 116 | Monitoring Crop Growth During the Period of the Rapid Spread of COVID-19 in China by Remote Sensing. IEEE Journal of Selected Topics in Applied Earth Observations and Remote Sensing, 2020, 13, 6195-6205. | 2.3 | 17 |
| 117 | Synergy of Active and Passive Remote Sensing Data for Effective Mapping of Oil Palm Plantation in Malaysia. Forests, 2020, 11, 858. | 0.9 | 17 |
| 118 | The land footprint of the global food trade: Perspectives from a case study of soybeans. Land Use Policy, 2021, 111, 105764. | 2.5 | 17 |
| 119 | Contrasting influences of biogeophysical and biogeochemical impacts of historical land use on global economic inequality. Nature Communications, 2022, 13, 2479. | 5.8 | 16 |
| 120 | Towards a global oil palm sample database: design and implications. International Journal of Remote Sensing, 2017, 38, 4022-4032. | 1.3 | 15 |
| 121 | Analyzing land use intensity changes within and outside protected areas using ESA CCI-LC datasets. Global Ecology and Conservation, 2019, 20, e00789. | 1.0 | 15 |
| 122 | Improved Mapping Results of 10 m Resolution Land Cover Classification in Guangdong, China Using Multisource Remote Sensing Data With Google Earth Engine. IEEE Journal of Selected Topics in Applied Earth Observations and Remote Sensing, 2020, 13, 5384-5397. | 2.3 | 15 |
| 123 | Identifying ecosystem service value and potential loss of wilderness areas in China to support post-2020 global biodiversity conservation. Science of the Total Environment, 2022, 846, 157348. | 3.9 | 15 |
| 124 | Suppression of vegetation in multispectral remote sensing images. International Journal of Remote Sensing, 2011, 32, 7343-7357. | 1.3 | 14 |
| 125 | Climate effects of the GlobeLand30 land cover dataset on the Beijing Climate Center climate model simulations. Science China Earth Sciences, 2016, 59, 1754-1764. | 2.3 | 14 |
| 126 | Exploring the potential role of feature selection in global land-cover mapping. International Journal of Remote Sensing, 2016, 37, 5491-5504. | 1.3 | 14 |

| # | Article | IF | CITATIONS |
|-----|--|------|-----------|
| 127 | Difficult to map regions in 30 m global land cover mapping determined with a common validation dataset. International Journal of Remote Sensing, 2018, 39, 4077-4087. | 1.3 | 14 |
| 128 | Spatial-temporal patterns of features selected using random forests: a case study of corn and soybeans mapping in the US. International Journal of Remote Sensing, 2019, 40, 269-283. | 1.3 | 14 |
| 129 | Improving 3-m Resolution Land Cover Mapping through Efficient Learning from an Imperfect 10-m Resolution Map. Remote Sensing, 2020, 12, 1418. | 1.8 | 14 |
| 130 | Recent expansion of oil palm plantations into carbon-rich forests. Nature Sustainability, 2022, 5, 574-577. | 11.5 | 14 |
| 131 | Parallel Multiclass Support Vector Machine for Remote Sensing Data Classification on Multicore and Many-Core Architectures. IEEE Journal of Selected Topics in Applied Earth Observations and Remote Sensing, 2017, 10, 4387-4398. | 2.3 | 13 |
| 132 | Exploring difference in land surface temperature between the city centres and urban expansion areas of China's major cities. International Journal of Remote Sensing, 2020, 41, 8965-8985. | 1.3 | 13 |
| 133 | Carbonaceous aerosol emission reduction over Shandong province and the impact of air pollution control as observed from synthetic satellite data. Atmospheric Environment, 2020, 222, 117150. | 1.9 | 12 |
| 134 | Efficient biosynthesis of nucleoside cytokinin angustmycin A containing an unusual sugar system. Nature Communications, 2021, 12, 6633. | 5.8 | 12 |
| 135 | Climate response to introduction of the ESA CCI land cover data to the NCAR CESM. Climate Dynamics, 2021, 56, 4109-4127. | 1.7 | 11 |
| 136 | Characteristics of Greening along Altitudinal Gradients on the Qinghai–Tibet Plateau Based on Time-Series Landsat Images. Remote Sensing, 2022, 14, 2408. | 1.8 | 11 |
| 137 | Cross-Regional Oil Palm Tree Detection. , 2020, , . | | 10 |
| 138 | A CNN-Based Self-Supervised Synthetic Aperture Radar Image Denoising Approach. IEEE Transactions on Geoscience and Remote Sensing, 2022, 60, 1-15. | 2.7 | 10 |
| 139 | Analysis and Simulation of Geomagnetic Map Suitability Based on Vague Set. Journal of Navigation, 2016, 69, 1114-1124. | 1.0 | 9 |
| 140 | Assessing and Improving the Reliability of Volunteered Land Cover Reference Data. Remote Sensing, 2017, 9, 1034. | 1.8 | 9 |
| 141 | Abnormal phosphorylation of tau protein and neuroinflammation induced by laparotomy in an animal model of postoperative delirium. Experimental Brain Research, 2021, 239, 867-880. | 0.7 | 9 |
| 142 | Accuracy comparison and driving factor analysis of LULC changes using multi-source time-series remote sensing data in a coastal area. Ecological Informatics, 2021, 66, 101457. | 2.3 | 9 |
| 143 | Construction Method of the Topographical Features Model for Underwater Terrain Navigation. Polish Maritime Research, 2015, 22, 121-125. | 0.6 | 8 |
| 144 | A Fully Automatic Method to Extract Rare Earth Mining Areas from Landsat Images. Photogrammetric Engineering and Remote Sensing, 2016, 82, 729-737. | 0.3 | 8 |

| # | Article | IF | CITATIONS |
|-----|---|-----|-----------|
| 145 | Harnessing synthetic biology-based strategies for engineered biosynthesis of nucleoside natural products in actinobacteria. Biotechnology Advances, 2021, 46, 107673. | 6.0 | 8 |
| 146 | A large-scale, long time-series (1984‒2020) of soybean mapping with phenological features: Heilongjiang Province as a test case. International Journal of Remote Sensing, 2021, 42, 7332-7356. | 1.3 | 8 |
| 147 | The Accuracy of Winter Wheat Identification at Different Growth Stages Using Remote Sensing. Remote Sensing, 2022, 14, 893. | 1.8 | 8 |
| 148 | Exploring the temporal density of Landsat observations for cropland mapping: experiments from Egypt, Ethiopia, and South Africa. International Journal of Remote Sensing, 2018, 39, 7328-7349. | 1.3 | 7 |
| 149 | Exploring intra-annual variation in cropland classification accuracy using monthly, seasonal, and yearly sample set. International Journal of Remote Sensing, 0, , 1-16. | 1.3 | 7 |
| 150 | Livestock farmers' perception and adaptation to climate change: panel evidence from pastoral areas in China. Climatic Change, 2021, 164, 1. | 1.7 | 7 |
| 151 | Towards an open and synergistic framework for mapping global land cover. PeerJ, 2021, 9, e11877. | 0.9 | 7 |
| 152 | Fast and robust detection of oil palm trees using high-resolution remote sensing images. , 2019, , . | | 7 |
| 153 | Mineral composition of the Martian Gale and Nili Fossae regions from Mars Reconnaissance Orbiter CRISM images. Planetary and Space Science, 2018, 163, 97-105. | 0.9 | 6 |
| 154 | Spatiotemporal crop NDVI responses to climatic factors in mainland China. International Journal of Remote Sensing, 2019, 40, 89-103. | 1.3 | 6 |
| 155 | Reducing human pressure on farmland could rescue China's declining wintering geese. Movement Ecology, 2020, 8, 35. | 1.3 | 6 |
| 156 | Sustainable Development Goals (SDGs) Priorities of Senior High School Students and Global Public: Recommendations for Implementing Education for Sustainable Development (ESD). Education Research International, 2022, 2022, 1-14. | 0.6 | 6 |
| 157 | Intermodality models in pan-sharpening: analysis based on remote sensing physics. International Journal of Remote Sensing, 2014, 35, 515-531. | 1.3 | 5 |
| 158 | Exploring the performance of spatio-temporal assimilation in an urban cellular automata model. International Journal of Geographical Information Science, 2017, 31, 2195-2215. | 2.2 | 5 |
| 159 | Exploring the addition of Landsat 8 thermal band in land-cover mapping. International Journal of Remote Sensing, 2019, 40, 4544-4559. | 1.3 | 5 |
| 160 | Multisource-Domain Generalization-Based Oil Palm Tree Detection Using Very-High-Resolution (VHR) Satellite Images. IEEE Geoscience and Remote Sensing Letters, 2022, 19, 1-5. | 1.4 | 5 |
| 161 | Evaluation of Future Impacts of Climate Change, CO2, and Land Use Cover Change on Global Net Primary Productivity Using a Processed Model. Land, 2021, 10, 365. | 1.2 | 5 |
| 162 | Coconut Trees Detection on the Tenarunga Using High-Resolution Satellite Images and Deep Learning. , 2021, , . | | 5 |

| # | Article | IF | CITATIONS |
|-----|---|-----|-----------|
| 163 | Nighttime lights, urban features, household poverty, depression, and obesity. Current Psychology, 2023, 42, 15453-15464. | 1.7 | 5 |
| 164 | Mapping spatial-temporal nationwide soybean planting area in Argentina using Google Earth Engine. International Journal of Remote Sensing, 2022, 43, 1724-1748. | 1.3 | 5 |
| 165 | On the Growth and Detectability of Land Plants on Habitable Planets around M Dwarfs. Astrobiology, 2017, 17, 1219-1232. | 1.5 | 4 |
| 166 | Semantic segmentation based large-scale oil palm plantation detection using high-resolution satellite images. , 2019, , . | | 4 |
| 167 | Exploring the correlations between ten monthly climatic variables and the vegetation index of four different crop types at the global scale. Remote Sensing Letters, 2017, 8, 752-760. | 0.6 | 3 |
| 168 | An Integrated Land Cover Mapping Method Suitable for Low-Accuracy Areas in Global Land Cover Maps. Remote Sensing, 2019, 11, 1777. | 1.8 | 3 |
| 169 | Coupled modelling and sampling approaches to assess the impacts of human water management on land-sea carbon transfer. Science of the Total Environment, 2020, 701, 134735. | 3.9 | 3 |
| 170 | Identifying Potential Cropland Losses When Conserving 30% and 50% Earth with Different Approaches and Spatial Scales. Land, 2021, 10, 704. | 1.2 | 3 |
| 171 | Automatic registration for ASAR and TM images based on region features. , 2007, , . | | 2 |
| 172 | Characteristics of Remote Sensing Emission Spectra of Composite Igneous Rocks. , 2008, , . | | 2 |
| 173 | Variational model-based very high spatial resolution remote sensing image fusion. Journal of Applied Remote Sensing, 2014, 8, 083565. | 0.6 | 2 |
| 174 | A sampling workflow based on unsupervised clusters and multi-temporal sample interpretation (UCMT) for cropland mapping. Remote Sensing Letters, 2018, 9, 952-961. | 0.6 | 2 |
| 175 | A structured approach to the analysis of remote sensing images. International Journal of Remote Sensing, 2019, 40, 7874-7897. | 1.3 | 2 |
| 176 | Matching area selection of an underwater terrain navigation database with fuzzy multi-attribute decision making method. Proceedings of the Institution of Mechanical Engineers Part M: Journal of Engineering for the Maritime Environment, 2019, 233, 1133-1140. | 0.3 | 2 |
| 177 | Cropland heterogeneity changes on the Northeast China Plain in the last three decades (1980s–2010s). PeerJ, 2020, 8, e9835. | 0.9 | 2 |
| 178 | Conjugate Gradient Method Neural Network for Medium Resolution Remote Sensing Image Classification. Communications in Computer and Information Science, 2011, , 264-270. | 0.4 | 2 |
| 179 | Domain adversarial neural network-based oil palm detection using high-resolution satellite images. , 2020, , . | | 2 |
| 180 | Global relative ecosystem service budget mapping using the Google Earth Engine and land cover datasets. Environmental Research Communications, 2022, 4, 065002. | 0.9 | 2 |

| # | Article | IF | CITATIONS |
|-----|---|-----|-----------|
| 181 | Open Geospatial Information Services Chaining Based on OGC Specifications and Processing Model. , 2008, , . | | 1 |
| 182 | A Standard Based Spatial Information Service Model for Adaptive Services Chaining. , 2008, , . | | 1 |
| 183 | A fast removal method of thin cloud/haze cover for optical remote sensing images based on multi-fractal. Proceedings of SPIE, 2011, , . | 0.8 | 1 |
| 184 | Network Security Evaluation Model Based on Cloud Computing. Communications in Computer and Information Science, 2012, , 488-495. | 0.4 | 1 |
| 185 | Oil palm modelling in the global land surface model ORCHIDEE-MICT. Geoscientific Model Development, 2021, 14, 4573-4592. | 1.3 | 1 |
| 186 | Evaluating the Farmland Use Intensity and Its Patterns in a Farming—Pastoral Ecotone of Northern China. Remote Sensing, 2021, 13, 4304. | 1.8 | 1 |
| 187 | Jujubecake: An Extension of LSTM Considering Correlation among Input Blocks. , 2020, , . | | 1 |
| 188 | Soybean EOS Spatiotemporal Characteristics and Their Climate Drivers in Global Major Regions. Remote Sensing, 2022, 14, 1867. | 1.8 | 1 |
| 189 | Implementation of data node in spatial information grid based on WS resource framework and WS notification. , 2006, , . | | 0 |
| 190 | Monitoring Land Subsidence by Using Multi-temporal Differential SAR Interferometry: A Use Case in Jiaxing, China. , 2008, , . | | 0 |
| 191 | Forward XPath rewriting over XML data streams. , 2009, , . | | 0 |
| 192 | A study of PS-InSAR method for small area urban land subsidence. , 2010, , . | | 0 |
| 193 | Urban-Expansion Driven Farmland Loss Follows with the Environmental Kuznets Curve Hypothesis: Evidence from Temporal Analysis in Beijing, China. Communications in Computer and Information Science, 2020, , 394-412. | 0.4 | 0 |
| 194 | Global Change of Land-Sparing and Land-Sharing Patterns over the Past 30 Years: Evidence from Remote Sensing and Statistics. Remote Sensing, 2021, 13, 5090. | 1.8 | 0 |
| 195 | A study of the serious conflicts between oil palm expansion and biodiversity conservation using high-resolution remote sensing. Remote Sensing Letters, 2023, 14, 654-668. | 0.6 | 0 |